

PROTON IRRADIATION FACILITY AT INR RAS LINAC

S. Gavrilov[†], S. Bragin, A. Feschenko, V. Gaidash, O. Grekhov, Y. Kalinin, Y. Kiselev, S. Lebedev, A. Melnikov¹, V. Serov, A. Titov¹, O. Volodkevich, Institute for Nuclear Research of the Russian Academy of Sciences, Moscow, Russia

D. Arbuznikov, O. Podgornaya, E. Prokhorov, S. Razinkov, P. Tsedrik, S. Tsibryaev, RFNC, All-Russian Research Institute of Experimental Physics, Sarov, Russia

¹ also at Moscow Institute of Physics and Technology (State University), Moscow, Russia

Abstract

A new proton irradiation facility to study radiation effects in electronics and different materials was constructed at INR RAS linac. The beam intensity range is 10^7 – 10^{12} protons per separate pulses up to 1 μ A of average beam current. The energy is adjusted by switching on/off the fields in accelerating cavities and with energy degraders in the range 20–210 MeV. Features of the facility development, in-air operation, diagnostics system, as well as experimental results of beam adjustment and test irradiation are presented.

INTRODUCTION

An accelerating complex based on a linear proton accelerator (linac) of Institute for Nuclear Research RAS is a multipurpose facility with a wide range of tasks for neutron research, radioactive isotope production and medical physics. In 2017 a new proton irradiation facility (PIF) was constructed to research proton irradiation induced effects in electronics, devices and materials.

A structural diagram of the linac is shown in Fig. 1. The main parts are: bending magnet with vacuum beam pipe, beam dump, target positioning system with energy degrader and beam diagnostic instrumentation. PIF is installed at the outlet of the linac in the 600 MeV beam energy area, where available bending magnet is used to deflect a beam from the linac axis by an angle of 7.5° for in air irradiation of targets.

PIF DESIGN AND MAIN PARAMETERS

Beam energy at the PIF is adjusted in the range 20–210 MeV by a switching off/on of accelerating cavities, which provide discrete energy values with a full energy spread $< 1\%$, for intermediate beam energy values an energy degrader should be used. However the presence of the degrader along with the outlet aluminium window with 1 mm thickness and 900 mm air gap leads to a significant increase of the energy spread, especially for low beam energies. Figure 2 shows an energy spectrum, calculated in TRIM [1], for a monoenergetic beam with 49 MeV initial energy after 4.6 mm aluminium degrader.

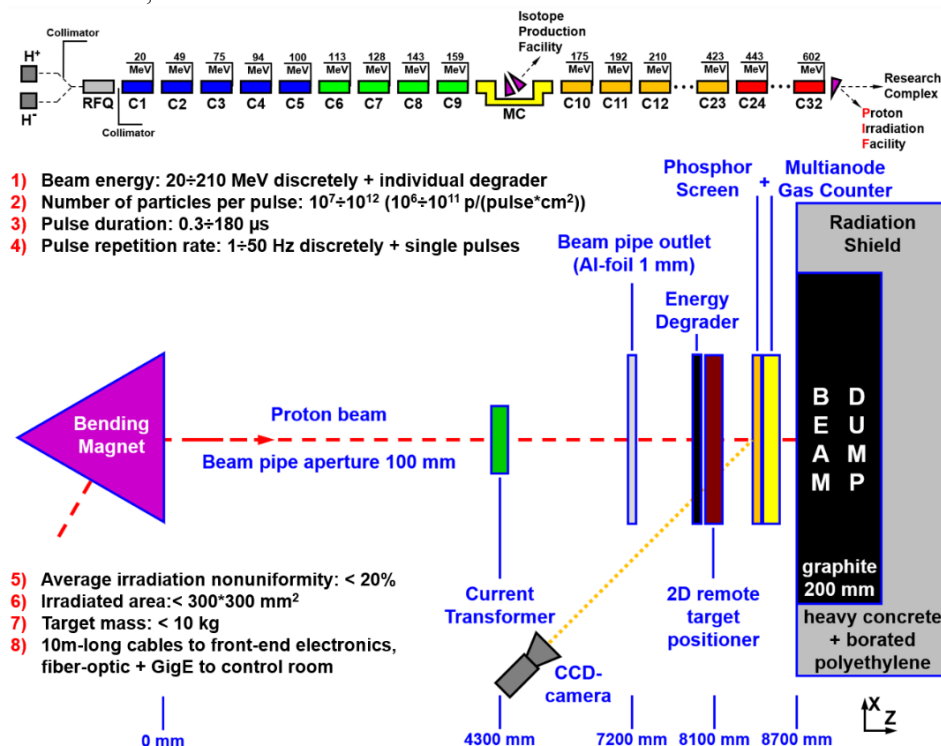


Figure 1: General layouts of the linac and proton irradiation facility at the outlet of the linac.

[†] s.gavrilov@gmail.com

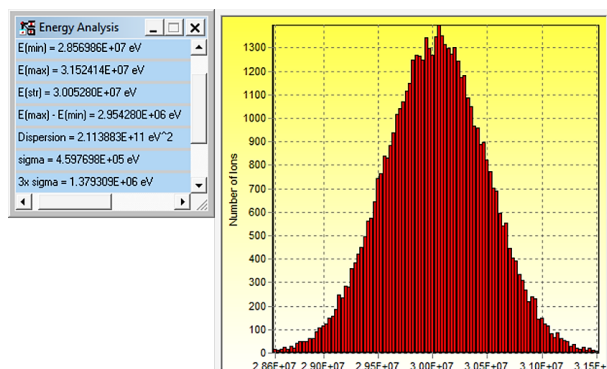


Figure 2: Beam energy spectrum of a monoenergetic beam with 49 MeV initial energy after 1 mm Al outlet window + 900 mm air gap + 4.6 mm Al energy degrader.

Beam intensity is defined by a combination of three parameters: pulse current, which can be controlled in the range 10^7 – 10^{12} protons per pulse by two collimators at the linac injection channel, pulse duration, variable in the range 0.3–180 μ s, and pulse repetition rate (1, 5, 10, 20, 25, 40, 50 Hz discrete mode plus single pulse count mode).

The two-dimensional target positioner (Fig. 3, point 3) provides a remote motion control of an irradiated target with the mass < 10 kg in the range ± 150 mm from the beam axis with a speed up to 100 mm/s.

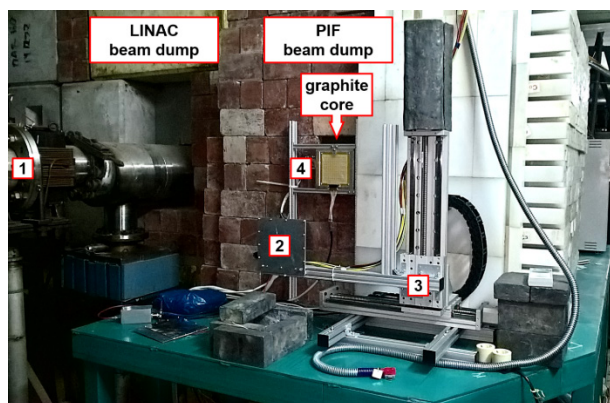


Figure 3: PIF installation. 1. Beam pipe outlet. 2. Beam energy degrader. 3. 2D target positioner. 4. Multianode gas counter with phosphor screen.

Beam Dump

The beam dump consists of a graphite core inside a shield of heavy concrete and borated polyethylene blocks. Preliminary simulations in SHIELD [2] show, that for a maximum foreseen beam average current 1 μ A at the energy 210 MeV the most intensive neutron fluxes (about 10^6 n/cm²/s) are generated in the up direction and sideways and should be absorbed totally by the linac tunnel shield consisted of 1.7 m heavy concrete and 7 m soil.

Simulations of the backward neutron flux from the dump at the target show, that the integral flux is less than 10% of neutron flux generated inside the target and these neutrons have an energy spectrum below 1 MeV, that is their influence on irradiation results at the PIF operating energies should be negligible.

BEAM DIAGNOSTICS

A multianode gas counter (MGC) was proposed initially as the main detector for low intensity diagnostics at the PIF.

Central region operates as an ionization chamber (Fig. 4) to count particles in a beam pulse. Ionization electrons move to the current electrode from both sides, forming a relative beam intensity signal.

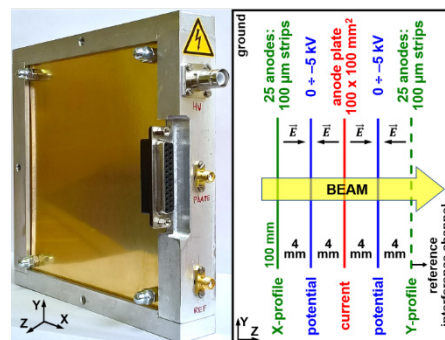


Figure 4: MGC photo and layout.

Lateral regions are proportional chambers for beam position and profile measurements. Each chamber is formed by the potential electrode and a multichannel structure, which consists of 25 anode strips with 100 μ m width, 100 mm length and 4 mm spacing. Strong non-uniform field around stripes leads to electron avalanches, increasing the desired signal.

A system of luminescent diagnostics was foreseen as alternative instrumentation to control beam position and profiles. It consists of a phosphor screen (PS) with 100 x 100 mm² operating area, fixed at the entrance plate of MGC (Fig. 5), and CCD-camera.

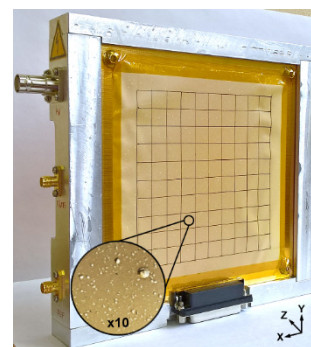


Figure 5: Phosphor screen fixed at MGC.

PS is made of P43 powder melted with polyimide – such process provides easy-to-use, but non-uniform luminescent film. However these nonuniformities of the powder are tens times smaller, than foreseen beam size. The light emitted by PS is registered by monochrome CCD-camera Basler acA780-75gm in 12-bit mode. In the actual PIF layout the reproduction PS scale is 2.2 pixel/mm.

Besides measurements of spatial transverse parameters PS can be used as a pulse particle counter due to a high linearity of P43 light yield as a function of incident particles number. Certainly, this type of intensity measurements, as well as MGC, demands a calibration by some absolute measurer, in our case – BCT.

BEAM TEST RESULTS

Beam tests were done in the full range of PIF parameters. The current range $10^{11} \div 10^{12}$ p/pulse is totally covered by BCT for current measurements and partially covered by PS for position, but not for profile and current measurements. It was shown, that the beam density $\sim 10^{10}$ p/cm² leads to PS light yield saturation. Besides, at peak beam currents about 10^{12} p/pulse and beam energies > 45 MeV, link through GigE interface was lost several times after $50 \div 100$ pulses with $1 \div 10$ Hz repetition rate.

MGC is also saturated in this current range and aging effects appear. The most important one is an irreversible decreasing of the signals from MGC stripes, which starts at beam density $> 10^{10}$ p/cm². At this density during beam tests the signals from the stripes started to decrease and disappeared totally at about 10^{11} p/cm². The main hypothesis about this effect is a sputtering of the gold from the nickel and following burning of the stripe in the avalanche due to O₂ molecular ions, that leads to a total stripe destruction and/or formation of dielectric oxide film on the stripe surface (Fig. 6), which blocks low energy ionization electrons.

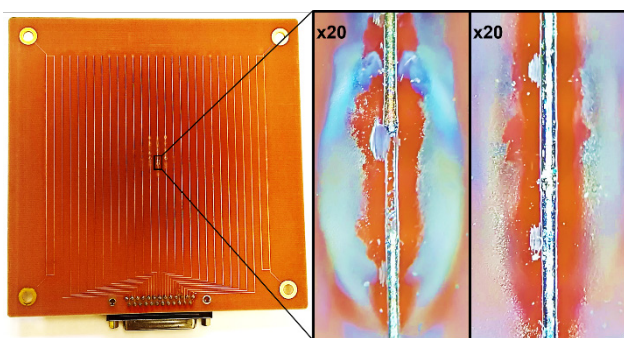


Figure 6: Aging effects at strips of proportional chamber: total stripe destruction and stripe oxidation – temper colors at the stripe nickel surface can be observed at the photos.

An initial procedure of calibration is started at about $100 \div 150$ μ A pulse current ($\sim 10^{11}$ p/pulse), when BCT signal-to-noise ratio is still good enough, and MGC with PS operate already without saturation. The experimental operational range of MGC is $10^7 \div 10^{11}$ p/pulse.

Beam profiles measurements with PS are routine. In this case, it is more precise instrument obviously, as provides ~ 1 mm resolution vs. 4 mm in MGC (Fig. 7).

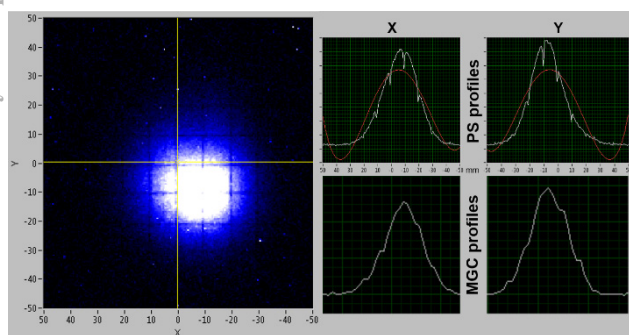


Figure 7: Beam cross-section at the PS and postprocessing profiles from the PS image and from MGC data.

Moreover, PS shows 2D beam cross sections and reveals images of irradiated targets with an ability to observe an internal density distribution (Fig. 8).

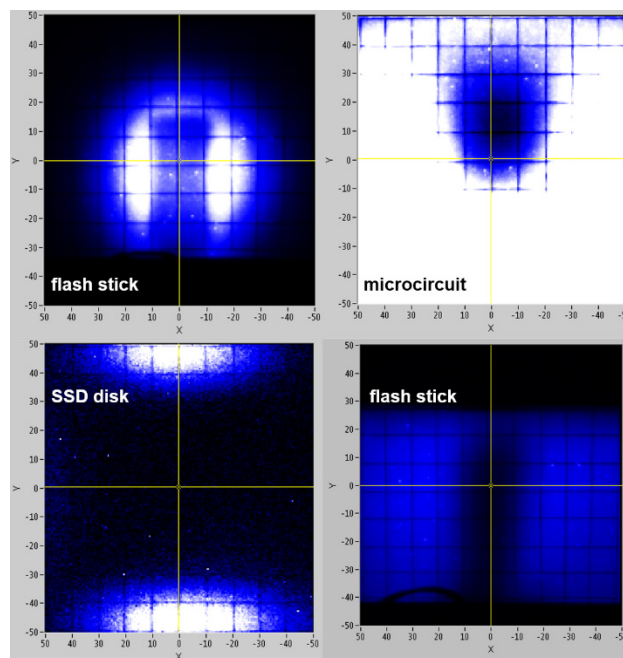


Figure 8: Images of “shadows” from beam irradiated objects at the phosphor screen.

After calibration a pulse particle count is also available by a software summation of image pixels intensities. The light yield remains linear in a full range of PS operation. However, a threshold sensitivity of PS is 10^7 p/cm², while MGC can provide both current and profile measurements with beam densities down to 10^5 p/cm² due to a special differential signal read-out with a reference interference channel.

CONCLUSION

A new proton irradiation facility was constructed at INR RAS linac. To provide the beam diagnostics in a full range of operation parameters three devices were used:

- beam current transformer – $10^{10} \div 10^{12}$ p/pulse,
- phosphor screen – $10^8 \div 10^{11}$ p/pulse ($10^7 \div 10^{10}$ p/cm²),
- gas counter – $10^7 \div 10^{11}$ p/pulse ($10^5 \div 10^{10}$ p/cm²).

Two test PIF runs were organized and confirmed preliminary simulations of beam dynamics with operating modes, limits of radiation shield, opportunities of diagnostic systems and target positioning system. The results of test operation show the necessity of the PIF diagnostics upgrade for a further optimization of the irradiation process.

REFERENCES

- [1] www.srim.org
- [2] <http://www.inr.ru/shield>